Int J Adv Manuf Technol (2013) 64:633–642
DOI 10.1007/s00170-012-4073-8

ORIGINAL ARTICLE

Analysis of the white layers formed during machining of hardened AISI 52100 steel under dry and cryogenic cooling conditions

Domenico Umbrello

Received: 3 October 2011 / Accepted: 19 March 2012 / Published online: 11 April 2012

Abstract The present work aims at understanding the effects of cryogenic coolant application and machined surface alterations during orthogonal machining of hardened AISI 52100 bearing steel. Experiments were performed under dry and cryogenic cooling conditions using cubic boron nitride tool inserts with varying initial hardness and tool shape. Several experimental techniques were used in order to analyze the machined surface. In particular, optical and scanning electron microscopes were used for characterizing the surface topography, whereas the microstructural phase composition analysis and chemical characterization have been performed by means of X-ray diffraction and energy-dispersive spectroscopy techniques. The experimental results prove that the white layer is partially reduced or can be totally eliminated under certain process parameters and cryogenic cooling condition.

Keywords Hard machining · Cryogenic cooling · White layer · AISI 52100 · SEM-EDS · XRD

1 Introduction

Metal cutting is associated with high temperatures at the tool-chip interface zone; and for this reason, the thermal aspect of the cutting process strongly affects the accuracy of the machining process including the machined product quality. The deformation process is concentrated in a very small zone and the local high temperatures due to heat generation have important consequences on both the tool and the workpiece; and the resulting microstructural alteration, often called the white layer formation, can be induced. Such an affected layer is generally considered to be detrimental to the life of machined component [1] since it has a significant impact on the magnitude of the maximum residual stresses and on the location of its compressive peak [2, 3]. This layer is typically a few tens of microns in thickness, hard, and brittle, and presents a relative resistance to etching and consequently, reaches a white appearance when observed by an optical microscope.

Numerous studies have been conducted on the white layer analysis during machining of hardened steels [1, 3–7]; only few were carried out on investigating the mechanisms related to white layer formation [8–11].

In addition, the convective cooling effect of cutting fluids on this affected layer has not yet been clarified [12]. Konig et al. [13] suggested suppression of white layers with coolants, Zurecki et al. [11] showed that cryogenic nitrogen spray cooling of cutting tool and tool–work contact limit the thickness of white layer, but others [14, 15] indicated no such effect.

Therefore, the objective of this paper is to verify which is the main cause for the while layer formation. Moreover, the proposed research permits to investigate the effect of cryogenic coolant system on white layer formation when AISI 52100 hardened steel is machined by cubic boron nitride (CBN) inserts. For this reason, an experimental campaign was carried out and several experimental techniques were used to analyze the machined surface. In particular, optical and scanning electron (SEM) microscopes were utilized for measuring the white layer thickness, micro-indentation Vickers tester, and infrared thermo-camera were used to respectively measure the hardness variation on the surface

D. Umbrello (✉)
Department of Mechanical Engineering, University of Calabria,
87036 Rende, CS, Italy
e-mail: d.umbrello@unical.it
URL: www.unical.it

D. Umbrello
Institute for Sustainable Manufacturing (ISM),
University of Kentucky,
Lexington, KY 40506, USA
e-mail: d.umbrello@uky.edu
URL: www.ism.uky.edu

and the whole thermal field. Finally, energy-dispersive X-ray spectroscopy (EDS) and X-ray diffraction (XRD) techniques were respectively used for chemical characterization and microstructural phase composition. The experimental results prove that the white layer observed on the machined surface of the hard turned specimens is the result of microstructural alteration, i.e., the generation of a martensitic structure.

2 Brief remarks on white layer formation in hard machining

The concept of "white layer" also called "phase transformed materials", "white phase", "nonetching layers", "white etching" etc., is not new and it refers to hard surface layers appearing white under the microscope and formed in a variety of ferrous materials under many different conditions [16]. The first approach to the study of the possible causes of the white layer was carried out in 1912 [17] when, analyzing the surfaces of used steel wire ropes, the formation of white etching layers was observed. Many efforts have been done in order to understand the mechanics of white layer formation and there is general agreement on stating that different types and forms of white layer have been observed depending upon the precise operating conditions and the materials used.

In sum, three main contributory mechanisms have been identified as responsible for white layer generation [18]:

1. the mechanism of surface reaction with the environment
2. the mechanism of severe deformation that produces a homogenous structure or one with a very fine-grained structure
3. the mechanism of rapid heating and quenching which results in transformation products

It has been suggested that any of these phenomena alone or in combination refines the subsurface microstructure of the worn specimens, specifically the grain size, to a point where it cannot be resolved optically [19].

The hypothesis of surface reaction with the environment was elaborated after founding white layer on worn surface. In such case, in fact, particular environments such as oxygen and nitrogen have been identified and several mechanisms of surface reaction have been suggested to prove it [20].

Sometime, it was hypothesized that both very large strain deformation (shear strain, >2 [21]) and strain rates are the principal factors contributing to the formation of this layer with ultrafine-grained or nanocrystalline structures [22]. Therefore, the mechanical effect has been explored as the possible dominant factor for the white layer formation. Mybokwere et al. [23], Cho et al. [24], and Zhang et al. [25] showed that dynamic recrystallization and recovery are the dominant processes in the formation of surface white layers and internal white adiabatic shear bands, which are

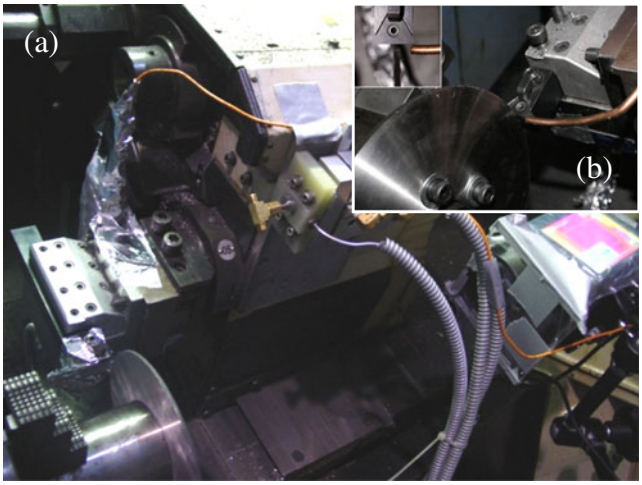

Fig. 1 **a** Experimental setup for orthogonal cutting tests and **b** nozzle position for cryogenic delivery

internal non-etching white bands in steels, deformed at high strain rates (from 10^3 to 10^6 s^{-1}).

Concerning the third possible mechanism of white layer formation, it is well known that temperatures in machining operations can reach high values causing microstructure modifications or austenitization in the case of ferrous alloys. Ramesh [10] also found that the influence of stress and strain on the austenite-start temperature of steels, due to high dislocation density associated with large strain, produces an approximate austenite-start temperature of 550–650 °C. Moreover, Barry and Byrne [8] and Chou and Evans [9] affirmed that the high austenite content of the surface white layer clearly confirms the occurrence of the reverse martensite transformation during machining. Mao et al. [26] investigated the affected layers formed in grinding of AISI 52100 steel. They found that the dominant factor determining the white layer formation during grinding of hardened steel grinding is the thermal effect. Such metallurgical change is due to the rapid increase in temperature, combined with high pressure generated by the action of the tool, transforming the machined surface to the austenitic state. When the tool leaves, the surface cools down and the critical speed of martensite formation is reached by

Table 1 Test conditions

Test	HRC	Cutting speed (m/min)	Feed rate (mm/rev)	Cooling methods	Tool shape
1	61.0±1	75	0.125	Dry	Honed
2	61.0±1			Cryogenic	Honed
3	56.5±1			Cryogenic	Honed
4	56.5±1			Cryogenic	Chamfered
5	54.0±1			Cryogenic	Honed
6	54.0±1			Cryogenic	Chamfered

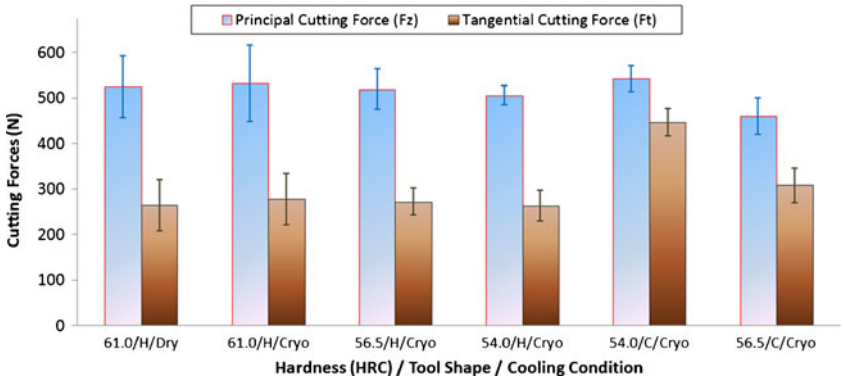

Fig. 2 Variation of cutting (Fz) and thrust (Ft) forces during machining under dry and cryogenic cooling conditions at varying initial material hardness, cooling system, and tool shape (*C* chamfer, *H* hone)

convection of heat into the air and by conduction into the workpiece material. As a result of the high thermal cooling (Chou and Evans [9] have estimated the surface cooling rate in hard turning to be of the order of 10^4 °C/s), some austenite has insufficient time to transform and some retained austenite traces can be found in the surface layer.

3 Experimental procedure

Disks of hardened *AISI 52100* steel (outer diameter, 150 mm; disk thickness, 1.4 mm) were prepared, machined, and heat-treated. Afterwards, a gentle grinding was required to restore flatness and parallelism after the distortion caused during quenching. During heat treatment, the disks were divided into three lots and different quenching and tempering treatments were used to through-harden the disks to different initial hardness levels: 54±1 HRC, 56.5±1 HRC, and 61±1, respectively.

Dry and cryogenic cutting tests were conducted on a stiff high-speed computer numerical control (CNC) lathe by means of orthogonal operation using CBN tool inserts mounted on a CTFNR3225P11 tool holder (providing a rake angle of −8°) which was held in a Kistler 9121 three-component piezoelectric dynamometer for measuring forces as illustrated in Fig. 1.

In order to avoid effects on the produces machined surface related to transient condition (in either feed or speed) due to the orthogonal configuration, the experiments were executed in the following sequence:

1. The disk was mounted in the mandrel held in the chuck of the CNC turning center (Fig. 1) and the cutting insert was mounted in the tool holder
2. The tool was aligned and brought close to the rotating workpiece by single-stepping through the CNC program (i.e., only one block/line of program code is executed with each press of the button by the operator)
3. All the instruments are set to "record" mode and the CNC program is taken out of single-step mode
4. With the next press of the button the rest of the program is executed uninterrupted—i.e., the tool enters the workpiece and continues cutting at the prescribed feed rate up till the prescribed end-of-cut diameter, and then instantaneously retracts at maximum feed. This insures that the rubbing of the tool against the final machined workpiece surface is minimal (though it may not be zero) and, equally importantly, invariant/constant for all the experimental conditions. Further, since the feed rate employed is in the low range (0.05–0.125 mm/rev) according to the tool makers, and due to the relatively large workpiece diameter (150 mm at start and 80 at the

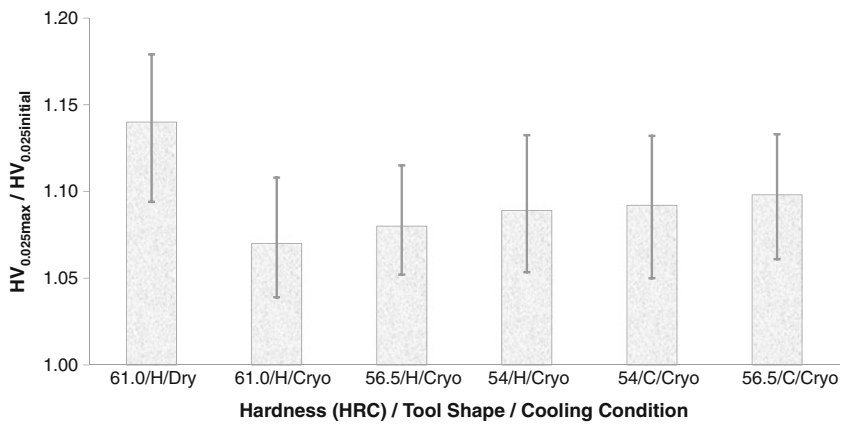

Fig. 3 Experimental surface hardness modification at varying initial material hardness, cooling system, and tool shape (*C* chamfer, *H* hone)

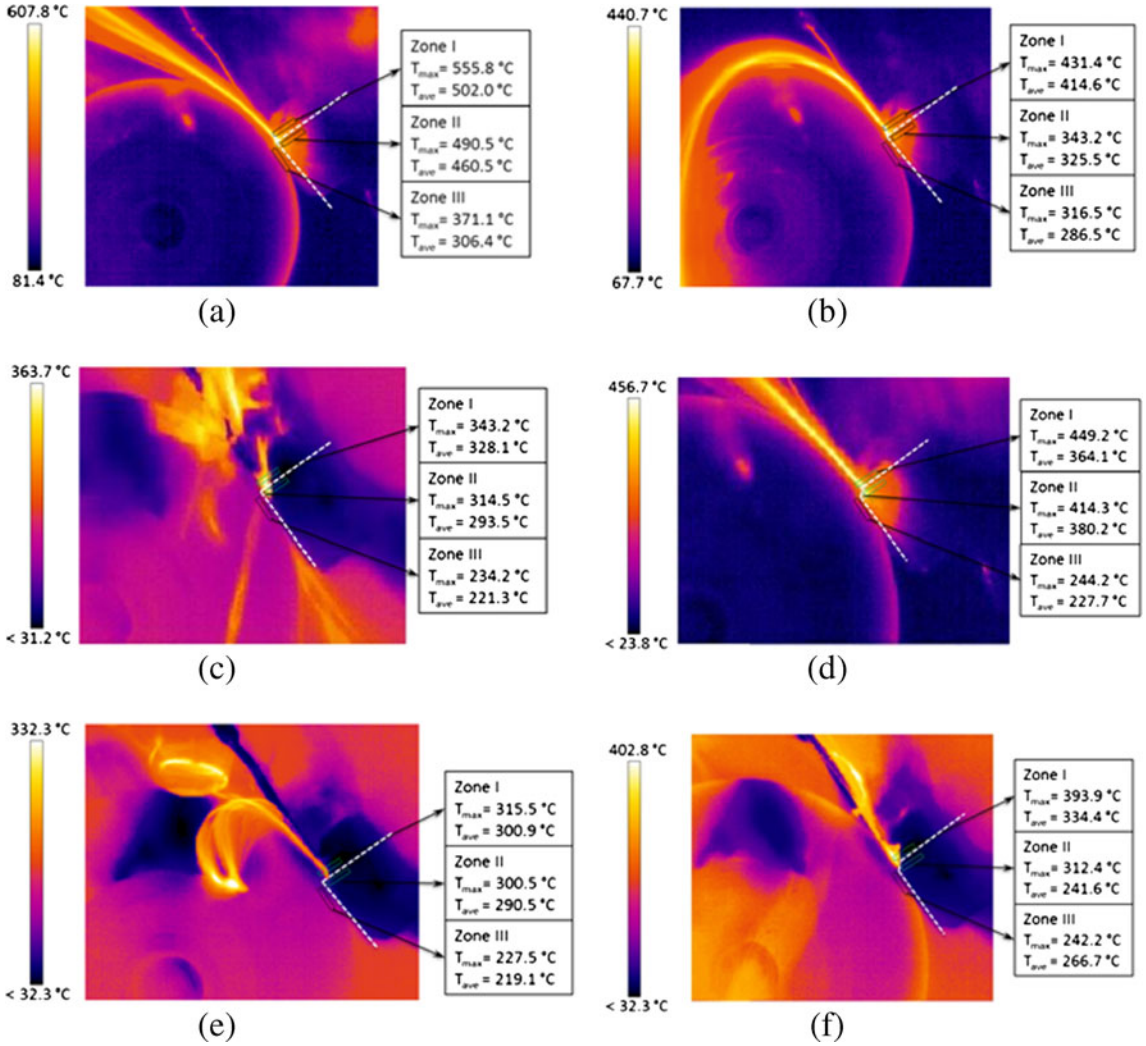

Fig. 4 Temperature fields in the three analyzed zones using dry and cryogenic cooling conditions: **a** test 1, **b** test 2, **c** test 3, **d** test 4, **e** test 5, **f** test 6

end) the rpm corresponding to the cutting speeds employed are also relatively low (159–298 rpm), it is possible for the CNC machine's hardware to change from radially inward feed to outward extraction almost instantaneously for all practical purposes. Hence, the transient effects were minimal, and this was confirmed from the force signals recorded during the cutting.

The disks were machined under dry and cryogenic cooling conditions for fixed cutting speed of 75 m/min and feed rate of 0.125 mm/rev, using low CBN content cubic boron

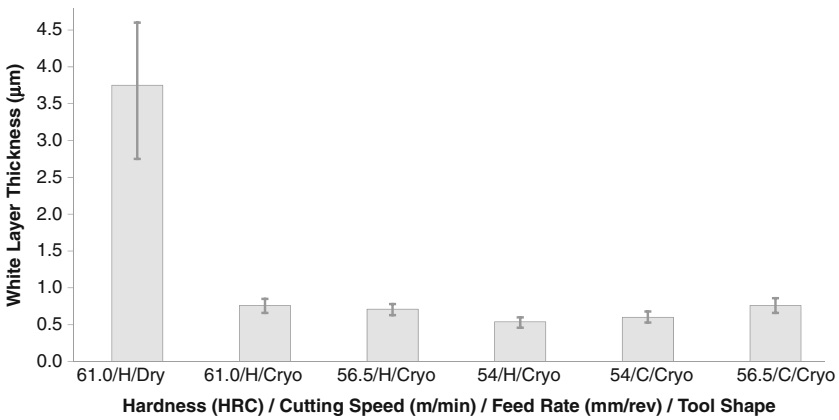

Fig. 5 Experimental white layer thickness at varying initial material hardness, cooling system and tool shape (*C* chamfer, *H* hone)

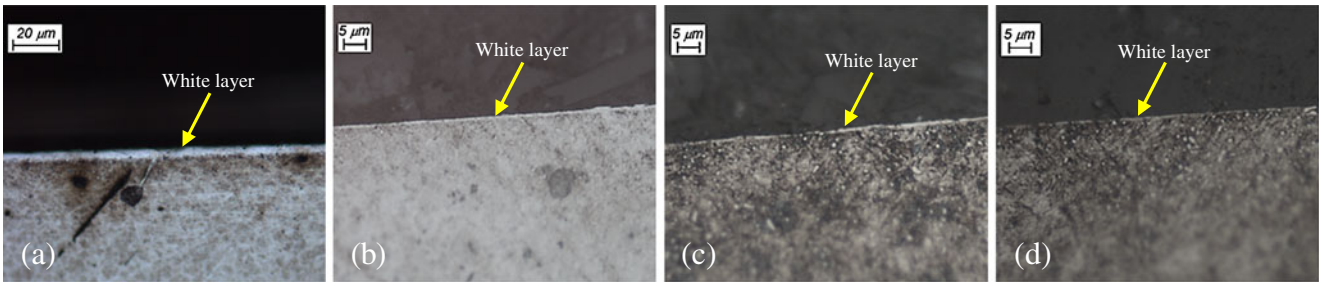

Fig. 6 Surface structures of the samples machined with honed edge tools observed by optical microscope: **a** test 1, **b** test 2, **c** test 3, **d** test 5

nitride tools (Seco grade: CBN 100) with two different edge geometries: chamfered (ISO TNGN 110308S with a chamfer of 20°×0.1 mm) and honed (ISO TNGN 110308E with an edge radius of 0.025 mm); the flank angle was −8°. An ICEFLY™ cryogenic equipment was used to provide liquid nitrogen as a cryogenic coolant during cryogenic cutting tests. Cryogenic coolant was applied by a nozzle to the area of interest as shown in Fig. 1; it is clear that cryogenic cooling heavily influences the results of machining process.

The cutting time of each test was 15–20 s in order to reach the mechanical and thermal steady state conditions. In such conditions, a flank wear of 0.03–0.05 mm was revealed on the utilized CBN tools. Due to this latter evidence, in this research, the influence of tool wear was not investigated. Table 1 shows the details of the experimental plan.

An infrared thermocamera was used during the experiments in order to detect the whole thermal field. The local workpiece emissivity was evaluated to be 0.21 and the transmission due to the external optic screen was estimated to be 0.5.

After machining, samples of 5×5 mm were sectioned by wire-EDM for microstructure analysis and microhardness measurements. Then, the samples were polished and etched for about 5 s using 5 % Nital solution to observe white layer using a light optical microscope (×1,000) and SEM. Microhardness was measured on the machined surface using a micro-indentation Vickers hardness tester with a certificated diamond indenter. Five measurements were made on the machined surface for each sample, with measurement locations well-spaced to avoid interference between indentations. The applied load of 25 g for 10 s was chosen in order to limit the indentation on the white layer itself avoiding any influence by the underlying layers.

An EDS was also performed in order to obtain elemental analysis of the machined surface. Finally, an XRD test gave the information about microstructural phase composition of the machined material. It was conducted by using X-ray equipment Bruker AXS D8 Discover with a quarter Ellurian cradle sample holder. The X-ray diffraction patterns were measured using CuK_α radiation (λ=1.54184 Å, $K_{\alpha1}/K_{\alpha2}$= 0.5) from a source operated at 40 kV and 40 mA. Samples were accordingly positioned at the center of plate into the X-ray goniometer in order to ensure a correct beam irradiation. The 2θ scans were carried out between 40 and 92 deg 2θ. The scan increment was 0.02°; the corresponding acquisition time was varied. Finally, estimation of the volume fractions of the retained austenite was carried out according to the ASTM E975 method [27, 28].

4 Experimental results and discussions

4.1 Cutting forces and surface microhardness

Figure 2 shows the trend of the average cutting forces for each experiment carried out when mechanical and thermal steady-state conditions were reached, while the error bars represents the standard deviations of the signal. The results highlight that the application of liquid nitrogen only has a slight influence on both cutting and thrust forces. On the other hand, the decrease of initial material hardness generally shows a slight decrease of the cutting forces for both dry

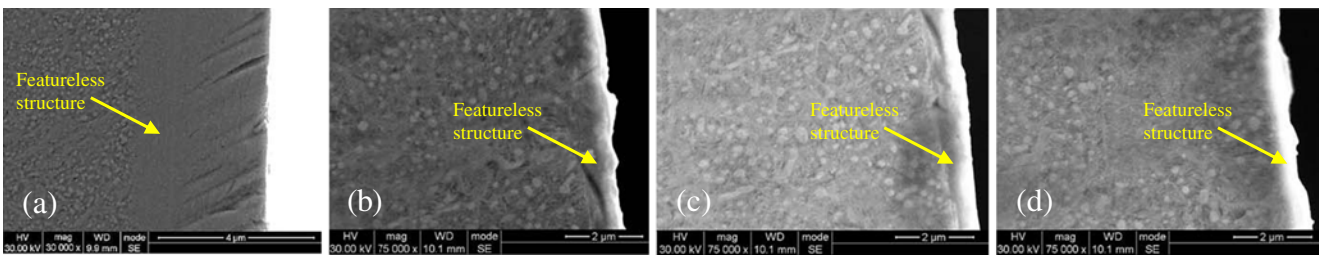

Fig. 7 SEM images of the samples machined with honed edge tools: **a** test 1, **b** test 2, **c** test 3, **d** test 5. The etching resistance of the turned white layer (featureless structure) is attributed to its nanograins structures due to dynamic recovery and recrystallization [8, 21]

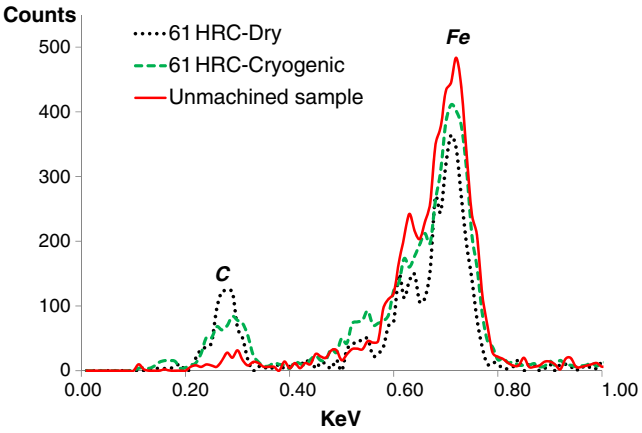

Fig. 8 Energy-dispersive spectroscopy (EDS) analysis on tests 1 (dry condition) and 2 (cryogenic cooling) vs. unmachined sample: 61 HRC, honed tool, V_c=75 m/min and f=0.125 mm/rev

and cryogenic conditions; also, cutting forces decrease when honed tool preparation was utilized. In contrast, the tangential cutting force increases when chamfer tools are used due to the higher effective rake angle.

Figure 3 shows the variation in microhardness values for the different experimental conditions employed. In particular, the results highlight that, in all of the investigated cases, the surface hardness is higher than that of the bulk material. Also, the value of the ratio $HV_{0.025}max/HV_{0.025}initial$ decreases when higher initial workpiece hardness as well as cryogenic cooling was selected. In contrast, the tool shape seems to be non-influential on $HV_{0.025}max/HV_{0.025}initial$ values when samples at 54 HRC as initial workpiece hardness were investigated, while the tool shape becomes an aspect to be taken into account when specimens with higher initial hardness were investigated. In fact, the use of chamfer tools during cryogenic machining of samples at 56.5 HRC produces higher values of the ratio $HV_{0.025}max/HV_{0.025}initial$.

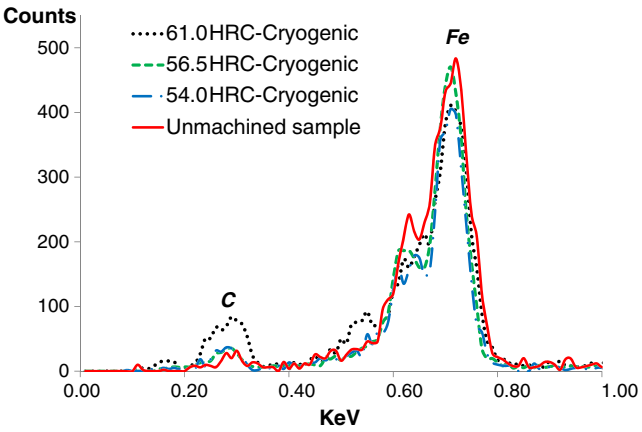

Fig. 9 Energy-dispersive spectroscopy (EDS) analysis on tests 2 (61 HRC), 3 (56.5 HRC) and 5 (54 HRC) vs. unmachined sample: cryogenic cooling, honed tool, V_c=75 m/min and f=0.125 mm/rev

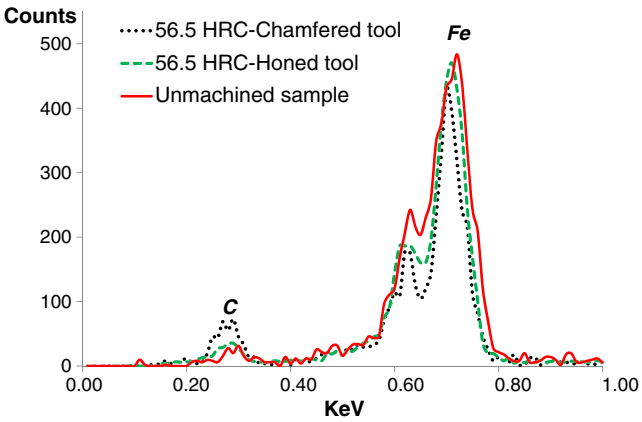

Fig. 10 Energy-dispersive spectroscopy (EDS) analysis on tests 3 (honed tool) and 4 (chamfered tool) vs. unmachined sample: cryogenic cooling, 56.5 HRC, V_c=75 m/min and f=0.125 mm/rev

These experimental observations are in agreement with those previously found by Poulachon et al. [22] as far the influence of initial hardness is concerned, and with those previously found concerning the influence of the tool shape [4]. In fact, it was demonstrated in [4] that the cutting tool with the chamfered edge produced a higher value of hardness at the surface than the tool with the honed edge during dry machining although the variation is slightly due to the different cooling methods used during experiments. In fact, it is worth pointing out that surface hardness modifications can be attributed either to rapid heating and quenching which results in microstructural transformation as well as to severe plastic deformation and consequently grain size refinement. Therefore, the lower temperatures reached during machining under cryogenic cooling condition can modify the cause of the white layer formation (i.e., mostly due to plastic deformation in cryogenic instead of thermal microstructural alteration in dry), determining this slight influence.

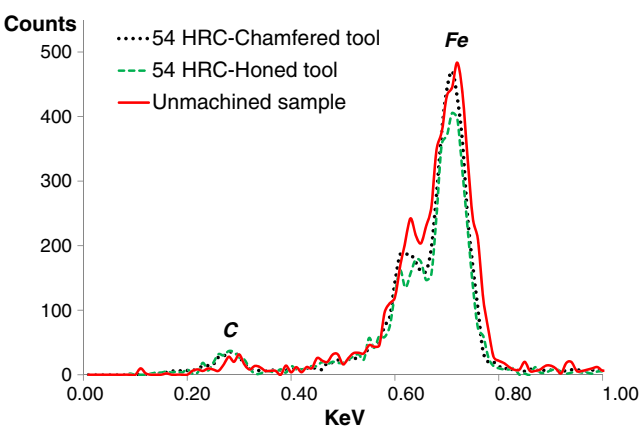

Fig. 11 Energy-dispersive spectroscopy (EDS) analysis on tests 5 (honed tool) and 6 (chamfered tool) vs. unmachined sample: cryogenic cooling, 54 HRC, V_c=75 m/min and f=0.125 mm/rev

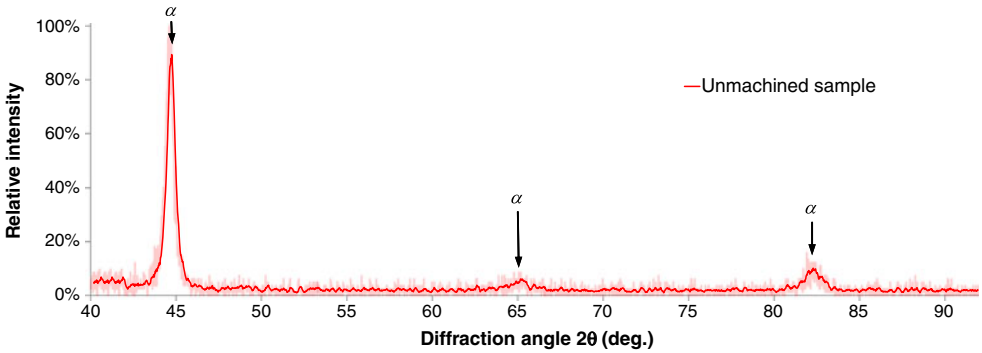

Fig. 12 X-ray phase analysis on specimen before machining operation (α ferrite-α)

4.2 Cutting temperatures

Comparison of the temperatures is often based upon the maximum temperatures measured on the tool rake face [29]. In this study, in order to have a more complete map of thermal profiles, different measurements were taken within the three zones shown in Fig. 4. More precisely, zone 1 is located on the tool chip interface, zone 2 is localized below the tool rake in correspondence of the primary shear plane (effect on the tool), while zone 3 is located on the machined surface downstream of the tool contact.

Figure 4 also shows, for the three different analyzed cutting zones, an evident decrease in both maximum and average temperatures when cryogenic coolant is used. It is evident, in fact, that the impact of cyro-jet cooling shows a reduction of the maximum temperatures in various zones ranging from 15 up to 50 %. Furthermore, the use of chamfered tool shape leads to an increase of both maximum and average temperature in the three zones. The reason is due to the higher rake angle near the primary and secondary shear zones (−28° instead of only −8° in the case of honed tool) which produces higher chip curvature, localized severe plastic deformation and, consequently, more mechanical work. Also, the initial workpiece hardness affects the measured temperature in the three zones, i.e., higher hardness leads to an increase of the temperature.

4.3 White layer

Figure 5 reports the experimental white layer thickness created by varying the initial workpiece hardness, cooling condition, and tool shape. In particular, the white layer ranges from less than 1 μm, when using cryogenic conditions to 4 μm during dry cutting as can be observed in optical micrographs (Fig. 6) and SEM images (Fig. 7) of the machined surfaces. Furthermore, the white layer decreases with reduced initial workpiece hardness; in contrast, only a slight influence of tool geometry on white layer thickness was found (Fig. 5). However, what is more important to highlight is that the white layer depth obtained using cryogenic cooling is much smaller than the white layer thickness measured when dry machining was performed. This significant difference was also observed by Zurecki et al. [11].

4.4 EDS analysis

Figure 8 depicts the data acquired by EDS analysis when specimens with 61 HRC were considered. As can be noted, higher carbon content (C) on machined surfaces was detected on specimens machined in dry condition as well as that using cryogenic cooling when compared to that observed on bulk material. The reason of higher carbon content in both machined specimens under different cooling conditions is related to the presence of retained austenite within the white layer. What is important to emphasize is that a lower carbon content was estimated on the machined surface under cryogenic cooling; that evidence is mostly due to the temperature reduction and consequently less microstructural transformation due to rapid heating and quenching.

The effect of cryogenic cooling on carbon content on machined surface becomes clear when specimens with lower hardness were investigated (i.e., lower white layer formation

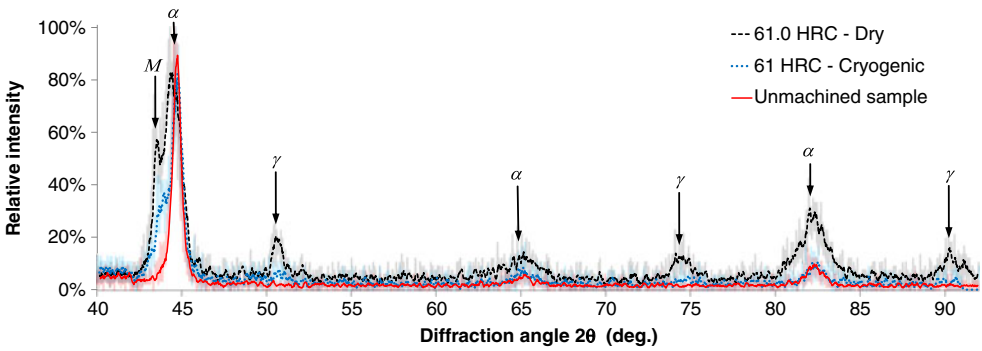

Fig. 13 X-ray phase analysis on tests 1 (dry condition) and 2 (cryogenic cooling) vs. unmachined sample: 61 HRC, honed tool, V_c=75 m/min and f=0.125 mm/rev (α ferrite-α, γ austenite, M martensite)

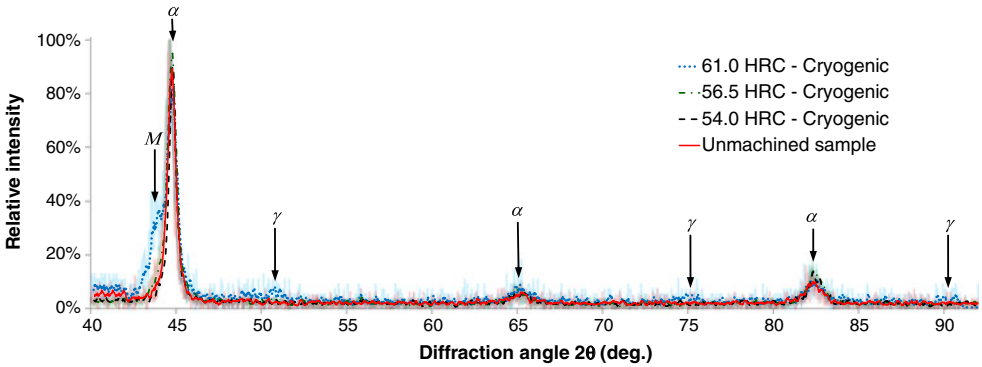

Fig. 14 X-ray phase analysis on Tests 2 (61 HRC), 3 (56.5 HRC) and 5 (54 HRC) vs. unmachined sample: cryogenic cooling, honed tool, V_c=75 m/min and f=0.125 mm/rev (α ferrite-α, γ austenite, M martensite)

as demonstrated in [4]). In fact, as can be observed in Fig. 9, the carbon content on the machined surface under cryogenic cooling was similar to that of the unmachined sample. Moreover, the use of cryogenic cooling on specimens with 54 and 56.5 HRC drastically reduced the presence of microstructural transformation due to rapid heating and quenching. In fact, it is worth noting that for similar cutting conditions, hardness, and tool edge preparation, but in dry condition, the carbon content detected on machined surface was higher than that measured on the bulk material [30].

It was found in a previous work [4] that the tool edge preparation also played a major role on the white layer formation when dry condition was utilized. This is partially confirmed when samples with 56.5 HRC were cryogenically machined (Fig. 10). In contrast, when cryogenic cooling is used on specimens with 54 HRC, the tool edge preparation seems to have no influence on white layer formation as shown in Fig. 11. Moreover, both the specimens, machined with identical process conditions but with different tool edges, show a similar carbon content of that measured on unmachined sample. This confirms that the application of cryogenic cooling on specimens with 54 HRC as initial hardness drastically reduced the presence of microstructural transformation due to rapid heating and quenching.

4.5 XRD analysis

Figure 12 shows the phase analysis obtained by means of X-ray diffraction technique on samples before the machining operation and, therefore, without the presence of the white layer on the investigated surface. In particular, the X-ray phase analysis on the unmachined surface of samples with different initial workpiece hardness evidences three peaks at 44.67°, 65.02°, and 82.33° which, according to Bragg's law and data reported in materials handbook [31], correspond to ferrite-α respectively at (110), (200), and (211) Miller's indices.

In contrast, when samples with 61 HRC as initial workpiece hardness machined under dry condition were investigated, the X-ray phase analysis shows several peaks (Fig. 13). Once again, three peaks are located at 44.67°, 65.02°, and 82.33° which correspond respectively to ferrite-α. What is more, four additional peaks can be found at 43.74°, 50.67°, 74.68°, and 90.67°. Specifically, peak at 43.74° in Fig. 13 corresponds to martensite while peaks at 50.67°, 74.68°, and 90.67°correspond to retained austenite respectively at (200), (220), and (311) Miller's indices as reported in materials handbook [32, 33] and found by Bragg's law. It is important to underline that these results are consistent with other experimental XRD observations [11, 20, 34].

In contrast, X-ray phase analysis conducted on sample machined under cryogenic cooling still shows the four peaks referred to the ferrite-α, whereas the peak related to martensite shows a lower relative intensity and those referring to the austenite are slightly higher (at 50.67° and 90.67°) or similar (at 74.68°) to those detected on the unmachined samples.

These experimental evidences confirm what EDS analysis have qualitatively showed, i.e., drastically reduction of white layer formation due to rapid heating and quenching

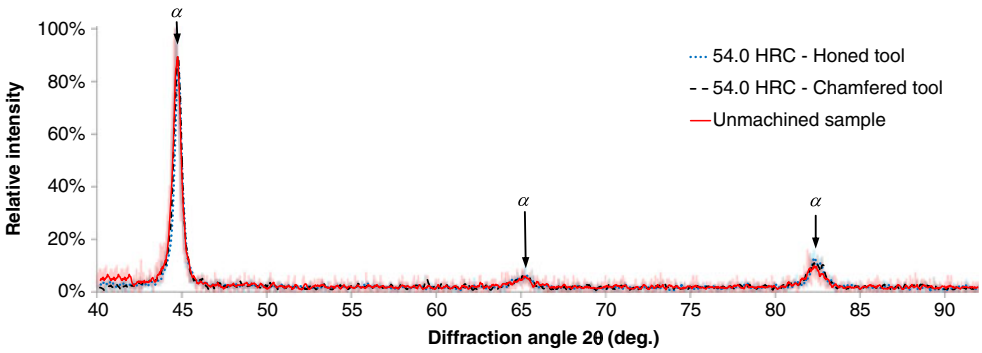

Fig. 15 X-ray phase analysis on tests 5 (honed tool) and 6 (chamfered tool) vs. unmachined sample: cryogenic cooling, 54 HRC, V_c=75 m/min and f=0.125 mm/rev (α ferrite-α)

(formation on untempered martensite structure). In fact, as it can be seen from Fig. 13, the relative intensity of the martensite peak from dry machining is significantly higher than the one from cryogenic machining. More precisely, the dry machining induced martensite peak is 168 % higher than the one from cryogenic machining.

Also, based on the relative peak areas (Fig. 13) and the procedures given in [27, 28], the volume fraction of retained austenite was also estimated based on the following equation:

$$\%\,\text{of RA} = \left(V_\gamma\right)\cdot 100 = \left(\frac{\frac{I_\gamma}{R_\gamma}}{\frac{I_\gamma}{R_\gamma}+\frac{I_\alpha}{R_\alpha}}\right)\cdot 100 \qquad (1)$$

where, R is a scale factor associated with phases and materials used, I is the calculated integrated intensity total for a phase, and V is the volume fraction of the phase. The austenite phase is represented by γ and the ferrite/martensite phase is represented by α. Thus, the calculated volume fraction of retained austenite (200) after dry and cryogenic machining are 4.5 and 1.9 % respectively, which indicates that cryogenic machining can significantly reduce the amount of retained austenite compared to dry condition.

The effect of cryogenic cooling on microstructural transformations on machined surface becomes more evident when samples with lower hardness were investigated (i.e., lower white layer formation as demonstrated in [4]).

In fact, as can be observed in Fig. 14, both the peaks referred to martensite and retained austenite (at (200), (220), and (311) Miller's indices, respectively), are drastically reduced or are not present when samples at 56.5 and 54 HRC were respectively machined under cryogenic condition. Therefore, it can be stated that the white layers observed for tests 3 and 5 (Table 1 and Fig. 5) are not due to rapid heating and quenching, with consequently untempered martensite formation, but are mainly due to severe plastic deformation and associated grain refinement.

Such evidence is also confirmed when samples at 54 HRC were cryogenically machined with the chamfered tool (Fig. 15). Also for test 6, both the peaks referred to martensite and retained austenite (200, (220), and (311)), are not present. Thus, it can conclude that tool geometry has no effect on white layer formation when samples at 54 HRC were cryogenically machined or it is limited when samples with higher initial workpiece hardness were taken into account as shown in Fig. 16.

5 Conclusions

Experimental observations reported in this investigation suggest that the use of cryogenic coolant significantly affects the thermal and mechanical aspects (i.e., temperatures, surface, hardness modification, microstructural changes, etc.) in machining of hardened AISI 52100. Cryogenic cooling influence is particularly evident when temperatures are analyzed and it leads to a reduction of microhardness values on the machined surface relative to dry cutting. It was also observed that the effectiveness of cryogenic machining in limiting white layer thickness; this is due to the lower temperatures reached during cutting, which limits or avoid martensitic phase changes.

Moreover, the performed EDS and XRD analysis show that the thermal effect was the main cause of the white layer formation in dry machining. In fact, the rapid heating and quenching on the surface creates an alteration with a consequent martensitic formation. In contrast, machining under cryogenic condition partially reduced or totally eliminated the microstructural changes due to rapid heating and quenching (i.e., the generation of a martensitic structure when hardened steels are considered).

Finally, it should be pointed out that other cutting conditions were not considered at this stage, and a further investigation on this topic will be necessary to better highlight exactly which cutting parameters (cutting speed, feed rate, initial workpiece hardness, etc.) should be chosen in order to improve the product's functional performance.

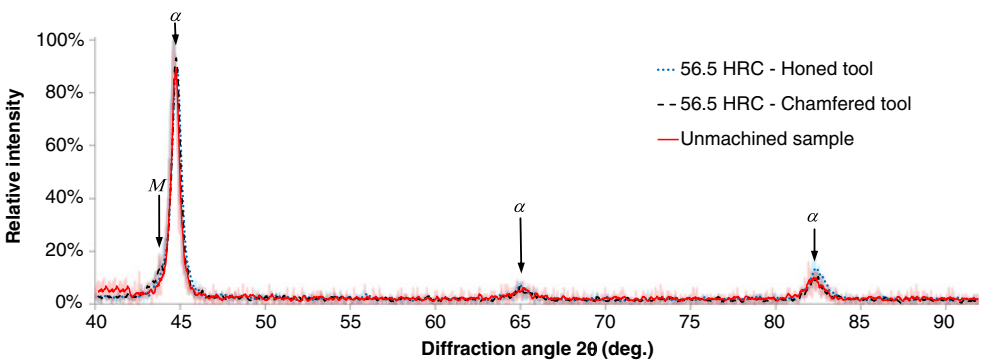

Fig. 16 X-ray phase analysis on tests 3 (honed tool) and 4 (chamfered tool) vs. unmachined sample: cryogenic cooling, 56.5 HRC, V_c=75 m/min and f=0.125 mm/rev (α ferrite-α, M martensite)

Acknowledgments The author gratefully thanks the Institute of Sustainable Manufacturing (University of Kentucky) for their support in developing the machining experiments and Mr. J. Backus from Kentucky Geological Survey for his help with the XRD measurements. The author also acknowledges Dr. R. M'Saoubi of Seco Tools AB for the donation of CBN cutting tools and tool holders.

References

1. Guo YB, Janowski GM (2004) Microstructural characterization of white layers by hard turning and grinding. Trans NAMRI/SME 32:367–374
2. Matsumoto Y, Hashimoto F, Lahoti G (1999) Surface integrity generated by precision hard turning. Ann CIRP 48(1–2):59–62
3. Ramesh A, Melkote SN (2008) Modeling of white layer formation under thermally dominant conditions in orthogonal machining of hardened AISI 52100 steel. Int J Mach Tools Manuf 48:402–414
4. Jayal AD, Umbrello D, Dillon OW Jr, Jawahir IS (2010) An investigation of the effects of cutting conditions, tool edge geometry and workpiece hardness on surface integrity in orthogonal machining of AISI 52100 steel. Trans NAMRI/SME 38:57–64
5. Ramesh A, Melkote SN, Allard LF, Riester L, Watkins TR (2005) Analysis of white layers formed in hard turning of AISI 52100 steel. Mater Sci Eng, A 390:88–97
6. Warren A, Guo YB, Weaver ML (2006) The influence of machining induced residual stress and phase transformation on the measurement of subsurface mechanical behaviour using nano-indentation. Surf Coat Technol 200:3459–3467
7. Chou YK, Evans CJ (1998) Process effects on white layer formation in hard turning. Trans NAMRI/SME 26:117–122
8. Barry J, Byrne G (2002) TEM study on the surface white layer in two turned hardened steels. J Mater Sci Eng A 25:356–364
9. Chou YK, Evans CJ (1999) White layers and thermal modeling of hard turned surfaces. Int J Mach Tools Manuf 39:1863–1881
10. Ramesh A (2002) Prediction of process-induced microstructural changes in orthogonal hard machining. Ph.D thesis, Mechanical Eng., Georgia Inst. of Technology
11. Zurecki Z, Ghosh R, Frey JH (2003) Investigation of white layer formed in conventional and cryogenic hard turning of steels. ASME International Mechanical Engineering Congress and Exposition, Washington, pp 16–21
12. Chou YK, Barash MM (1995) Review on hard turning and CBN cutting tools, 1st Int. Machining and Grinding Conference, SME Technical Paper MR 95–214, Dearborn, Michigan, pp. 949–962
13. König W, Klinger M, Link R (1990) Machining hard materials with geometrically defined cutting edges—field of applications and limitations. Ann CIRP 57(1):61–64
14. Berktold A, König W, Liermann J, Winands N (1994) Top-quality components not only by grinding. Ind Diam Rev 54(562):127–132
15. Tonshoff HK, Brandt D, Wobker HG (1995) Potential and limitation of hard turning, 1st Int. Machining and Grinding Conference, SME Technical Paper MR 95–215 Dearborn, Michigan, pp. 965–978
16. Poulachon G, Albert A, Schluraff M, Jawahir IS (2005) An experimental investigation of work material microstructure effects on white layer formation in PCBN hard turning. Int J Mach Tools Manuf 45(2):211–218
17. Stead JW (1912) Micro-metallography and its practical application. J West Scot Iron Steel Inst 19:169–204
18. Griffiths BJ (1985) White layer formations at machined surfaces and their relationship to white layer formations at worn surfaces. J Tribol 107:165–171
19. Wang Y, Lei T, Liu J (1999) Tribo-metallographic behavior of high carbon steels in dry sliding III. Dynamic microstructurals changes and wear. Wear 231:20–37
20. Klocke F, Brinksmeier E, Weinert K (2005) Capability profile of hard cutting and grinding processes. Ann CIRP 54(2):22–45
21. Akcan S, Shah S, Moyal SP, Chhabra PN, Chandrasekar S, Yang HTY (2002) Formation of white layers in steels by machining and their characteristics. Metall Mater Trans A 33(A):1245–1254
22. Poulachon G, Moisan A, Jawahir IS (2001) Tool-wear mechanisms in hard turning with polycrystalline cubic boron nitride tools. Wear 250:576–586
23. Mybokwere CO, Nutt SR, Duffy J (1994) Shear band formation in 4340 steel: a TEM study. Mech Mater 17:97–110
24. Cho KM, Lee S, Nutt SR, Duffy J (1993) Adiabatic shear band formation during dynamic torsional deformation of an HY-100 steel. Acta Metall Mater 41(3):923–932
25. Zhang B, Shen W, Liu Y, Tang X, Wang Y (1997) Microstructures of surface white layer and internal white adiabatic shear band. Wear 211:164–168
26. Mao C, Zhou Z, Zhang J, Huang X, Gu D (2011) An experimental investigation of affected layers formed in grinding of AISI 52100 steel. Int J Adv Manuf Technol 54:515–523
27. American Society for Testing and Materials International-ASTM E975-00 (2003) Standard practice for X-ray determination of retained austenite in steel with near random crystallographic orientation. 03.01, W. Conshohocken, PA
28. Pappas N (2006) Calculating retained austenite in steel post magnetic processing using X-ray diffraction, B.S. Undergraduate mathematics exchange 4(1):9–14
29. Davies MA, Cooke AL, Larsen ER (2005) High bandwidth thermal microscopy of machining AISI 1045 steel. Ann CIRP 54 (1):63–66
30. Umbrello D, Rotella G (2012) Experimental analysis of the mechanisms related to white layer formation during hard turning of AISI 52100 bearing steel. Mater Sci Technol 28(2):205–212
31. Joint Committee on Powder Diffraction Standards (1980) Powder diffraction file. Inorganic 6–10:150
32. Joint Committee on Powder Diffraction Standards (1988) Powder diffraction file. Inorganic 31–32:209
33. Joint Committee on Powder Diffraction Standards (1990) Powder diffraction file. Inorganic 35–36:283
34. Han S, Melkote SN, Haluska MS, Watkins TR (2008) White layer formation due to phase transformation in orthogonal machining of AISI 1045 annealed steel. Mater Sci Eng, A 488(1–2):195–204